From Pickering foams to porous carbonate materials: crack-free structuring in drying ceramics
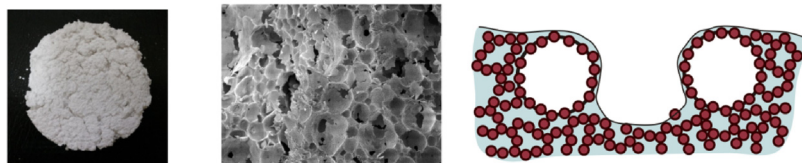
M. Hristova[a], I. Lesov[a], S. Tcholakova[a,*], V. Goletto[b], N. Denkov[a]

[a] Department of Chemical and Pharmaceutical Engineering, Faculty of Chemistry and Pharmacy, Sofia University, 1 J. Bourchier Ave., 1164 Sofia, Bulgaria
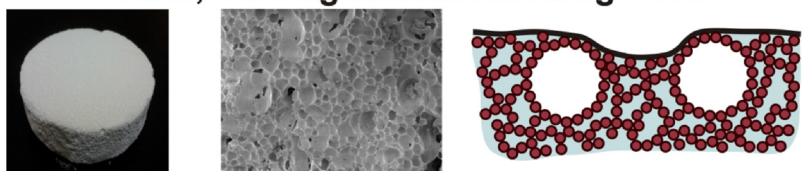[b] Saint Gobain Recherche, 39 quai Lucien Lefranc, 93303 Aubervilliers, France

GRAPHICAL ABSTRACT

ARTICLE INFO

ABSTRACT

Particle-stabilized foams have attracted considerable research interest, due to their long term stability (months to years) and the possibility to use them as precursors for production of porous materials with hierarchical porosity. In our previous study [Lesov et al., *J. Colloid Interface Sci.* 504 (**2017**) 48–57] we clarified the role of the rheological properties of the foamed suspensions and the type of foam film stabilization in the production of porous silica materials with low mass density and excellent insulating properties. In the current study we extend our approach to prepare lightweight carbonate ceramics with controlled density, shrinkage and good mechanical properties. To prepare the wet foam precursors, we tested a series of eight anionic surfactants which were previously reported to provide sufficient hydrophobization of $CaCO_3$ particles and long-term stability of the liquid foams. From those surfactants, the medium-chain fatty acids led to crack-free porous materials with superior mechanical strength, compared to the conventional surfactants. We study the reasons for the formation of cracks in drying Pickering foams and, on this basis, propose optimal conditions for obtaining dry porous carbonate materials with required porosity. Mechanistic explanations are proposed for the main observed effects.

* Corresponding author.
   E-mail addresses: mk@lcpe.uni-sofia.bg (M. Hristova), lesov@lcpe.uni-sofia.bg (I. Lesov), SC@LCPE.UNI-SOFIA.BG (S. Tcholakova), valerie.goletto@saint-gobain.com (V. Goletto), nd@lcpe.uni-sofia.bg (N. Denkov).

1. Introduction

Porous ceramics is a class of materials which is usually characterized with low mass density and high specific surface area. These properties make the porous ceramics desirable materials for vast range of applications, spanning from simple construction blocks to highly efficient catalyst supports, and even scaffolds for tissue engineering. Advantageous method for their preparation is the direct foaming technique, in which a concentrated particle suspension is foamed, dried and often sintered [1–3].

Gonzenbach et al. [4] showed that choosing appropriate surfactant and tuning its concentration, boosts the foaming of suspensions of hydrophilic particles. One recommendation for selection of appropriate surfactant in terms of foam stability is to use surfactants with an electrical charge opposite to that of the particles [4,5]. Such oppositely charged surfactants adsorb on the particles surface and modify *in situ* the particle hydrophobicity during foaming [4]. Some moderate particle hydrophobicity is considered as a prerequisite for particle adsorption on the surface of the foam bubbles and for ensuring the desired long-term stability of the formed Pickering foams [5–23].

Studies related to flotation industry, generation of hydrophobic coatings and stabilization of Pickering foams revealed that several anionic surfactants are suitable for (partial) hydrophobization of carbonate particles [24–30]. Thus, Somasundaran and Agar [24] showed that sodium dodecyl sulfate (SDS) is appropriate for the modification and flotation of calcite particles. Hana and Anazia [25–27] used carboxylic acids and their salts for similar purpose. Later on, other authors used oleic acid [28,29], dioctyl sodium sulfosuccinate (AOT) [30], and alkylbenzene sulfonic acid [31].

Zhou et al. [29] used the knowledge on carbonate modification to prepare Pickering foams in presence of oleic acid. The obtained wet foams were stable to coalescence and Ostwald ripening but suffered from water drainage, due to the relatively low concentration of carbonate particles and the respective low yield stress of the suspension. Similar results were obtained by Cui et al. [30], who used SDS and AOT for the surface modification of carbonate particles. However, the foams in [30] had low air fraction (e.g. below 50 vol. %), also contained particles with low concentrations and suffered from water drainage which made them inappropriate precursors for preparation of lightweight porous materials [32–34].

In our previous studies [33,34], we established that a well-defined, optimal ratio between the particle and surfactant concentrations may ensure very stable foam precursors. On one side, the surfactant content should be sufficiently high to partially hydrophobize the particles and to trigger their adsorption on the bubble surface during foaming. The particle hydrophobization should provide also moderate attraction between the neighboring particles to induce an optimal yield stress of the foamed suspensions which can stabilize the foams to drainage [20,33,34]. On the other hand, the surfactant concentration had to be sufficiently low to avoid the severe particle aggregation into large clusters and strong gels which would suppress the suspension foamability [33,34] and cause cracking in the drying foams [33–35].

The major aim of the current study is to apply the approach from [33,34] and to prepare carbonate ceramic materials with controlled porosity and optimal mechanical strength by selecting the most appropriate type and concentration of surfactant in the foamed carbonate suspensions. To achieve this aim we compare the effects of eight anionic surfactants, most of which have been reported previously to provide sufficient hydrophobization of $CaCO_3$. We found that particularly appropriate for formation of dry porous materials of high quality are the medium-chain fatty acids with 8 to 10 carbon atoms. The reasons for the formation of severe cracks in the drying carbonate foams are studied and explained mechanistically.

2. Materials and methods

2.1. Materials

We used $CaCO_3$ particles, provided as dry commercial powder (Omyabrite® 1300 X – OM, Omyacorp), containing 98 wt% calcium carbonate, 1 wt% humidity and 1 wt% insoluble salts. The average size of the particles provided by the manufacturer is 2.4 μm and the BET surface area is 25-30 m^2/g (ISO 9277). The mass density of the particles is 2700 kg/m^3.
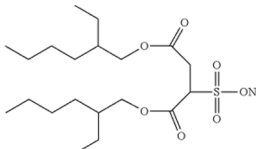
The anionic surfactants, listed in Table 1, were used to modify the particles' surface and to assist the suspension foaming. The conventional surfactants (viz. all except the fatty acids) were first prepared as 10 wt% stock solutions, while the fatty acids were used as received. Decanoic and dodecanoic acid were melted first (1 min at 50–60 °C) and then added to the suspensions.

All suspensions and surfactant solutions were prepared with deionized water, produced by Elix 3 module (Millipore, USA).

2.2. Suspension preparation

Suspensions with 30 wt% particle concentration were prepared in the following way: 180 g $CaCO_3$ particles were measured in a polyethylene jar and 420 g deionized water was added. This mixture was hand shaken and then placed on a rotating mill (BML-2, Witeg) for 10 min at 100 rpm. Afterwards, the suspension was homogenized for 3×10 min with a pulse sonicator (SKL1500-IIDN, Ningbo haishu sklon developer). The latter was set to 1 s long pulses with power output of 1200 W, followed by 0.5 s off, using a sonotrode with diameter of 20 mm. The suspension was then left to cool down to room temperature

Table 1
List of surfactants studied.

Name	In text	Chemical Formula	Producer	Average molecular weight, g/mol	Active content, %
Sodium α-olephin sulfonate	α-OS	$(C_nH_{2n^-1})SO_3Na$ (n ≈ 15)	AAKO	314.0	90
Sodium dodecyl sulfate	SDS	$CH_3(CH_2)_{11}SO_4Na$	Acros	288.4	99
Linear alkylbenzene sulfonate	LAS	$C_6H_5CH(C_nH_{2n+1}) SO_3Na$ (n ≈ 11.8)	Sigma	348.5	90
Dioctyl sodium sulfosuccinate	AOT		Sigma-Aldrich	444.6	99
Sodium lauryl ether sulfate	SLES	$C_{12}H_{25}(OCH_2CH_2)_3SO_4Na$	Stepan Co.USA	420.5	70
Octanoic acid	C8Ac	$C_7H_{13}COOH$	Fluka	144.2	99
Decanoic acid	C10Ac	$C_{10}H_{21}COOH$	Alfa Aesar	172.3	98
Dodecanoic acid	C12Ac	$C_{13}H_{27}COOH$	Acros	200.3	99

and used in the foaming experiments.

2.3. Wet foam preparation and foam stability assessment

Planetary mixer (Kenwood Chef Premier KMC 560, 1000 W) was used for suspension foaming. 250 g of 30 wt% carbonate suspensions were measured in a transparent, graduated mixing bowl and a given amount of surfactant solution was added. The surfactant concentration was calculated and is reported below with respect to the water volume in the foamed suspension.

The mixer was, first, set to a minimum speed for 2 min to homogenize the surfactant-particle mixture without generating foam. Then highest mixing speed was applied for 600 s or until a desired air volume fraction, Φ, was reached. Afterwards, the mixer was stopped and foam samples were taken for gravimetric determination of Φ and for characterization of the foam stability with respect to liquid drainage, bubble Ostwald ripening, and foam drying.

The foam stability upon drying was determined with 114 ml foam samples, placed in a custom made cylindrical Teflon molds (d = 7.5 cm and h = 2.6 cm). Foam samples were dried in an oven at 60 $\pm$ 10 °C, at ambient humidity.

The structure of the dried porous material was observed with Scanning Electron Microscopy (SEM) instrument TESCAN LYRA3 GM, Czech Republic. For these observations, the dried samples were broken into pieces and a small piece with approximate projection 2×2 cm^2 was taken from the middle of the sample and coated with Au/Pd alloy via high-vacuum sputter coating.

2.4. Mechanical strength of the dry materials

A stainless steel ball with known radius and mass was carefully placed on the surface of the porous material. Under the force of gravity, the ball penetrates into the solid porous material until the mechanical strength of the substrate balances the gravitational force exerted by the ball. We measured the diameter of the formed indentation dimple, a, and then calculated its area. The compressive strength of the porous material, σ_{Cr}, was calculated using a force balance, as explained in Supplementary section S1:

$$\sigma_{Cr} = \frac{mg}{2\pi R \left(R - \frac{1}{2}\sqrt{4R^2 - a^2} \right)} \tag{1}$$

Here g = 9.81 m/s^2 is the acceleration of gravity, while m and R are the ball mass and radius, respectively. The method was tested against commercial testing machine and gave practically the same results for materials without visible macroscopic cracks (see *ESI section S1*).

2.5. Supernatant preparation for measurement of the solution surface tension, particle zeta potential, and for performing model experiments with evaporating drops

Carbonate suspensions containing 30 wt % particles ± surfactant were prepared, homogenized and then centrifuged for 1 h at 5500 rpm and 25 °C (Sigma Laborzentrifugen 3–16 PK, Rotor 12,151). The separated supernatant was decanted and its surface tension was measured as a function of time using the pendant drop method on instrument DSA 10 (KRÜSS, Germany).

The zeta potential of the carbonate particles was measured with Zetasizer Nano ZS instrument (Malvern, UK). For these measurements, 0.1 wt% of the carbonate sediment was re-dispersed in the supernatant solution and at least 3 separate samples were measured, with an average of 100 runs per sample.

We used the supernatant with the re-dispersed particles, prepared as explained above for the zeta potential measurements, as a model system to study also the drying process on a microscale. We placed 1–2 μL droplets of supernatant + particles on a glass substrate and monitored

the water evaporation and the particle motion and aggregation in the drying drop by optical microscopy in transmitted light. We used microscope Axioplan (Zeiss, Germany), equipped with long-distance objectives Zeiss LD Epiplan 50×/0.50 and EC Plan-Neofluar 2.5x/0.075.

3. Experimental results and discussion

In this section we present experimental results about the preparation of wet foams, their drying and the mechanical properties of the dry porous materials, comparing the different surfactants. Afterwards, model experiments, aimed at explaining the observed differences in the mechanical strength of the final porous materials, are presented and discussed.

3.1. Preparation of the wet foams

One of our aims is to develop a robust procedure for preparation of lightweight carbonate materials with porosity > 90%. To calculate the fraction of air bubbles that we needed to entrap in the wet foam precursor, we used the relation derived in ref. [32]:

$$Porosity = 1 - \frac{\rho_{PM}}{\rho_{CaCO_3}} = \left[1 - \frac{\rho_{wall}(1 - \Phi)}{2700} \right] \tag{2}$$

where ρ_{PM} is the mass density of the final porous material, ρ_{CaCO_3} = 2700 kg/m^3 is the mass density of the carbonate material, ρ_{wall} is the mass density of the material containing closely packed solid particles after suspension drying, and Φ is the bubble volume fraction in the wet foam. We measured ρ_{wall} = 780 $\pm$ 50 kg/m^3 via drying of non-foamed suspension without surfactant. Thus we calculated that $\approx$ 65 vol. % bubbles should be trapped in the wet foams to obtain 90% porosity of the final dry material (see *ESI section S2*).

The suspension in absence of added surfactant did not generate foam within one hour of mixing due to the natural hydrophilic character of the CaCO$_3$ particles (contact angle with water < 15°) [30,36]. Therefore, to modify the particles and to assist foaming, we tested the surfactants listed in Table 1. Illustrative results for the kinetics of foaming of carbonate suspensions with decanoic acid (C10Ac) are presented in Fig. 1A. Low concentration of C10Ac allows the formation of a small amount of foam, but it does not reach the required 65% of bubble volume fraction even after a very long foaming time. Upon addition of C10Ac of moderate concentration, 7 mM, a steady process of foam generation is observed. Around 44 vol % air was entrapped within the first 10 min of mixing and the foam gradually increased up to $\approx$ 74 vol% after 40 min. At higher concentration of C10Ac, 29 mM, the foaming was much faster and Φ = 74% was reached in 8 min.

All studied surfactants, except for dodecanoic acid (C12Ac), had similar behavior at 7 mM – high foamability with foam formation within minutes. Air volume fraction $\geq$ 0.70 was typically reached within 600 s of mixing (Fig. 1C).

It is worth noting that, similarly to our previous study with silica suspensions, the surfactant concentrations triggering high foamability, i.e. $\Phi \geq 0.65$, corresponds to very low surface coverage of the particles by surfactant molecules. Estimates, using the known particle surface area and the amount of surfactant added to the suspension, show that $\approx$ 0.38 μmol/m^2, corresponding to $\approx$ 4.4 nm^2 per C8Ac molecule (assuming that all added C8Ac molecules are adsorbed) were sufficient to obtain stable foams. This value corresponds to less than 4% surface coverage of the particles, when assuming dense monolayer of $\approx$ 0.2 nm^2 per C8Ac molecule [28], specific surface area of the particles of 25 m^2/g, and adsorption of all surfactant molecules on the particles surface. The latter assumption was verified experimentally for C8Ac, but is not true for the conventional surfactants - see Section 3.3 below.

On the other hand, we observed that dodecanoic acid (C12Ac) did not affect the foamability of the carbonate suspensions within the entire concentration range tested (Fig. 1B). The most probable explanation of
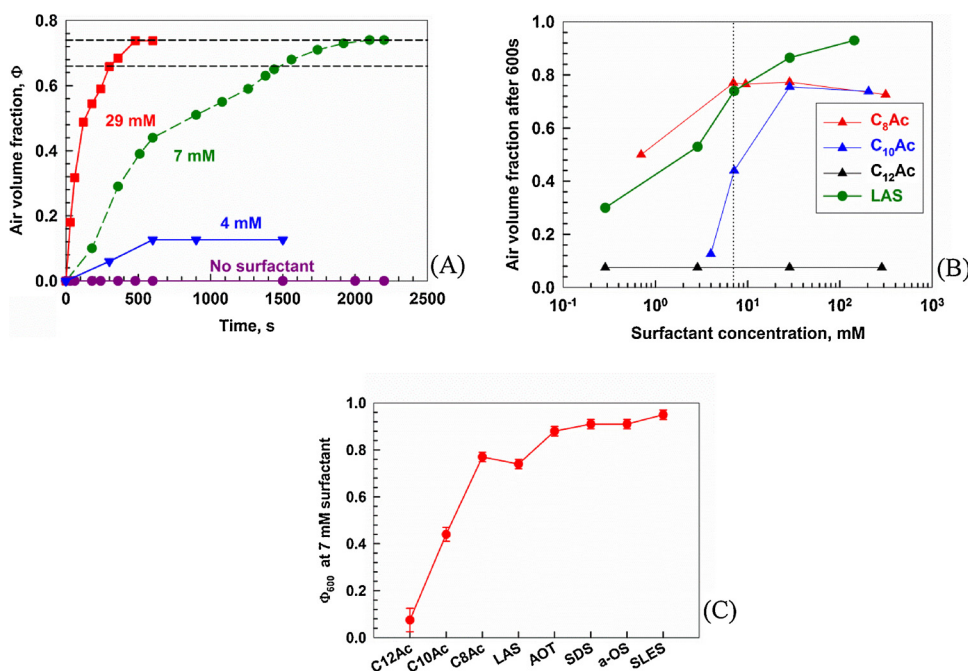
Fig. 1. (A) Kinetics of foam formation of 30 wt % carbonate suspension + decanoic acid with concentration, as indicated in the figure. Horizontal line at $\Phi = 0.65$ represents the required bubble volume fraction, above which the foams have sufficiently high air content for preparation of lightweight materials. (B) Φ after 600 s of mixing for octanoic (C8Ac), decanoic (C10Ac) and dodecanoic (C12Ac) acids, and for linear alkyl-benzene sulfonate (LAS). (C) Air volume fractions of foams after 600 s of mixing at 7 mM concentration, for different surfactants.

this result is the formation of calcium soaps, $Ca(C12Ac)_2$, which have very low solubility product, $pK_{sp} \approx 11.94$ [37]. As a result, C12Ac molecules precipitate and are not available to modify the particles surface. In addition, the calcium soaps of this type are known to have strong antifoam effect [38].

Our next aim was to compare the efficiency of the different surfactants with respect to their ability to yield stable porous materials. To reduce to a minimum the amount of surfactant needed and to avoid the particle aggregation in the suspension which has a negative effect on the stability of the final porous material [33], we make this comparison at the lowest surfactant concentration allowing the formation of voluminous foams. Thus, we foamed suspensions containing 7 mM surfactant and took samples for drying at air volume fraction, $\Phi = 0.65 \pm 0.02$ and $\Phi = 0.75 \pm 0.02$. We studied the stability of these wet foams upon drying, as well as the mechanical properties of the final dry porous materials.

All wet foams were stable to drainage. Some limited bubble Ostwald ripening was observed in the foams containing SLES, while all other foams showed no signs of bubble ripening. No bubble-bubble coalescence events were seen either. Reflected light images from the surface of the foams, taken immediately after the foam preparation, revealed that the foams films were stabilized by carbonate particles (see Fig. 2). Only in the foams with SLES surfactant we observed 5 to 10% of foam films which were partially stabilized by surfactant molecules – see the black foam film area, shown by arrow on the SLES image in Fig. 2. The presence of such thin black film areas could explain the limited bubble Ostwald ripening in the SLES-containing foams, as the air transfer between bubbles is inversely proportional to the foam film thickness.

In ref. [34] we showed that the type of foam film stabilization (by particles or by adsorbed surfactant molecules) plays an important role on the mechanical properties of the porous materials with high air volume fraction. We demonstrated that silica foams with $\Phi \approx 0.70$, whose films were stabilized by adsorbed surfactant molecules, had up to two times lower mechanical strength, compared to the foams with particle stabilized foam films. Based on the previous results obtained with silica foams, we might expect that all foams shown in Fig. 2, except those prepared in the presence of SLES, should have similar mechanical properties. However, we observed a significant difference in the mechanical strength of the porous carbonate materials. This effect and the reasons for its appearance are discussed in the following

sections.

3.2. Effect of surfactants on the mechanical strength of the dry carbonate materials

To compare the effect of surfactants on the mechanical strength of the porous materials, we used the procedures described in Sections 2.3–2.4. We prepared dry porous materials from foamed suspensions, containing 30 wt% particles and 7 mM surfactant, with air volume fractions $\Phi = 0.65$ and 0.75. The obtained porous materials were with average mass densities of $180 \pm 20 \, kg/m^3$ and $120 \pm 10 \, kg/m^3$, respectively. Illustrative pictures of the materials with $120 \, kg/m^3$ mass density are shown in Fig. 3. All these foams dried in "one piece", without visible cracks on their upper surface. However, once we flipped the porous samples over, we observed a lot of macroscopic cracks on their bottom surface (no such differences were seen with the silica foams in [34]). Only the materials prepared with fatty acids did not exhibit such macroscopic cracks on any of their surfaces.

Since these cracks did not allow us to compare the mechanical strength of the materials directly using standard tests with compressing machine (some of the samples fell apart upon touching), we used a stainless steel ball to measure their mechanical strength locally on their upper surface. Direct comparison showed that the method with the steel ball yields very similar results as the commercial testing machine (Tiratest 2300, Tira GmbH) for the materials without cracks (e.g. C8Ac), and it gave somewhat higher crushing stress for the ones containing macroscopic cracks.

Experimental results for the mechanical strength of the materials, prepared with different surfactants, are presented in Fig. 4A. Materials with $\rho = 120 \, kg/m^3$ and containing the surfactants SDS, AOT and α-OS had a compressive strength $\approx 3 \, kPa$. In comparison, the materials with C8Ac and C10Ac had much higher mechanical strength $\approx 13 \, kPa$. This significant effect of the C8Ac and C10Ac, as compared to the other surfactants, was observed with all samples tested, including those with higher mass density of $180 \, kg/m^3$, as shown for two of the surfactants in Fig. 4B.

We note that the indentation method probes the surface layer of the porous material and that the mass density of the surface layers of the different samples could deviate significantly from the average mass density of the materials (see Section 3.3 for further discussion of this
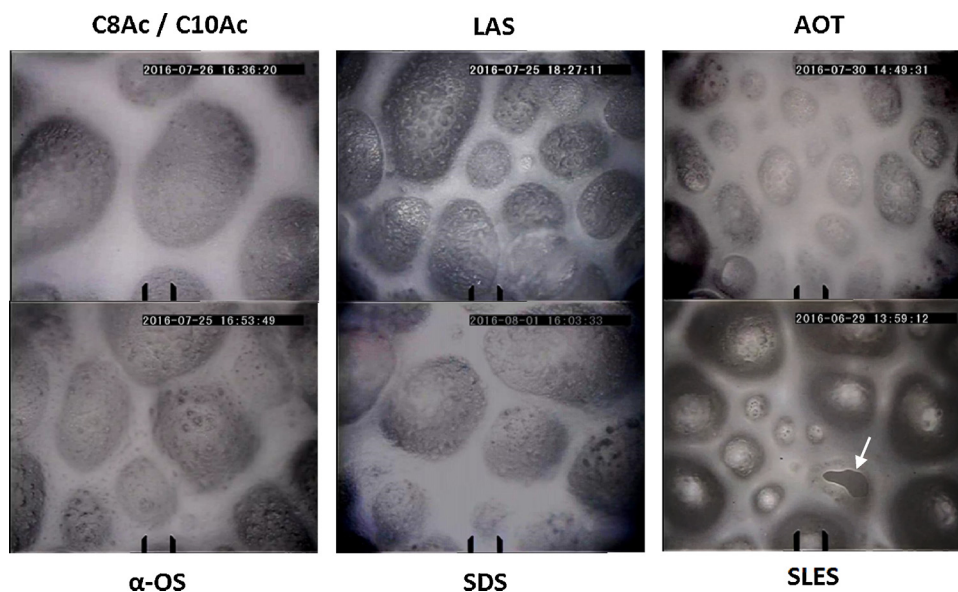
Fig. 2. Reflected light images of the bubbles on the surface of wet foams, immediately after their preparation. Foams contain 30 wt% particles, 7 mM surfactant, as indicated in the figure and 75 ± 2 vol.% air. Scales - 50 μm. The white arrow shows a foam film, stabilized by SLES surfactant.

issue). Therefore, for some systems we compared the "local" strength of the materials, measured by the steel ball, to their macroscopic strength measured by compressing machine, cf. the empty and full symbols in Fig. 4A. Similar results were obtained from both tests for the materials obtained with fatty acids, whereas for the materials obtained with other surfactants we measured higher strength locally at the upper surface in comparison to the macroscopic strength.

SEM micrographs of these materials evidenced that the lower mechanical stability of the samples is related to the presence of multiple micro-to-millimeter-sized cracks all along the materials bottom surface and in the adjacent bulk regions (see Fig. 4C-E).

To clarify the role of the air bubbles and of the rate of water

evaporation during drying on the process of crack formation, we performed several additional series of experiments. First, we dried non-foamed suspensions, containing 7 mM octanoic acid or sodium dodecyl sulfate (SDS) at 60 °C, under conditions equivalent to those used for drying the foamed suspensions. In these experiments we observed cracks at the bottom of the final dry materials in the presence of both octanoic acid and SDS, although these cracks were much smaller for octanoic acid in comparison to SDS-containing samples. When we made similar experiments with aerated suspensions, containing different volume fractions of bubbles, we found that even 20 vol.% bubbles are sufficient to prevent the crack formation in the presence of octanoic acid (but not in the case of SDS). These results clearly show that the
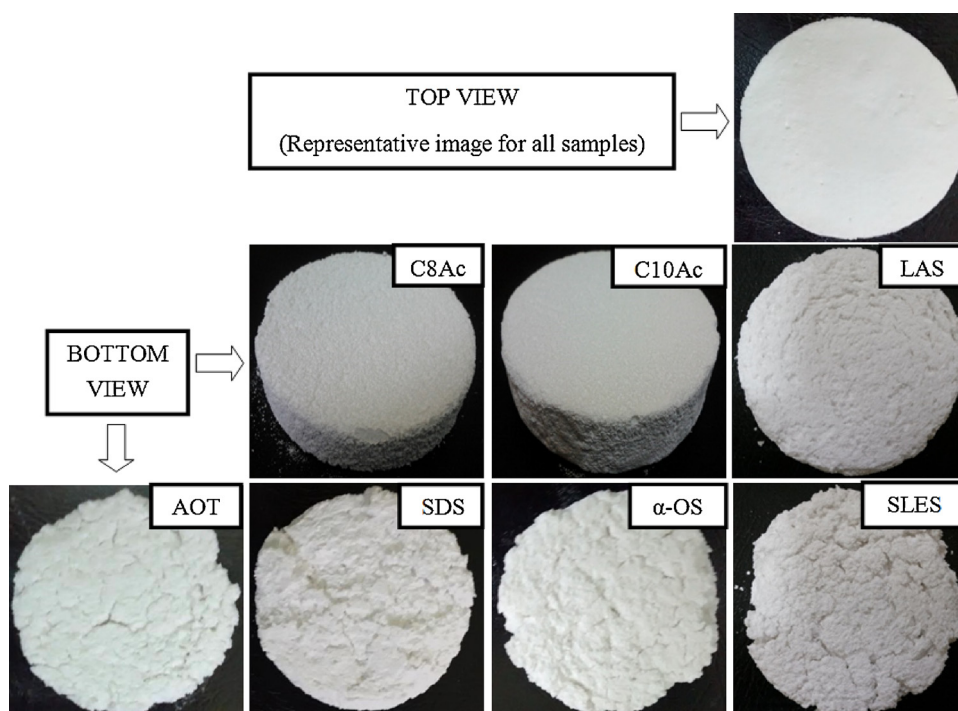

Fig. 3. Pictures of dried materials, prepared from wet foams containing 30 wt% particles and 7 mM surfactant (as indicated in the figure) at Φ = 0.75 ± 0.02. Foams were dried in Teflon molds with volume of 114 ml at 60 ± 10 °C and ambient humidity.
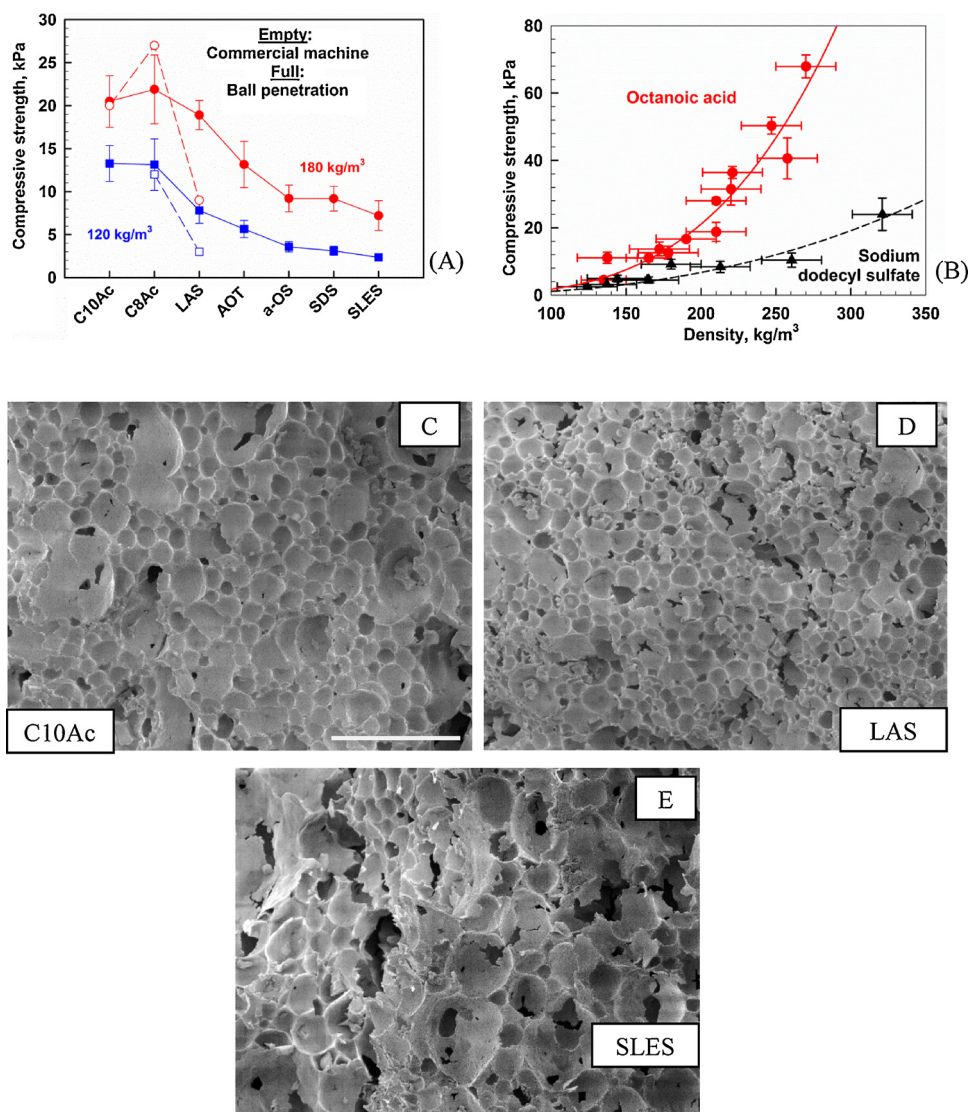
Fig. 4. **(A)** Mechanical strength of porous materials with different mass densities, as indicated in the figure. The error created by variations in the mass density of the materials was estimated to be ± 4 kPa for 180 kg/m³ and less than 2 kPa for 120 kg/m³ (see *ESI section S1*). **(C-E)** SEM pictures of dry foams, with density 180 ± 20 kg/m³: **(C)** C10Ac, **(D)** LAS and **(E)** SLES. Scale bar is 1 mm.

bubbles dispersed in the drying carbonate suspensions are not the cause of the cracking process (unless they are with very high volume fraction) – on the contrary, they suppress cracking. This latter conclusion is in agreement with literature results showing that the presence of deformable entities (drops, bubbles) inside drying suspension layers could adsorb/disperse the mechanical stress in-between the particles and, thus, suppress the cracking during drying of the suspension layer (see e.g. Jin et al. [39])

The mass density of the dry carbonate suspension, obtained without cracks in the presence of octanoic acid, was measured to be ρ_{wall} = 745 ± 50 kg/m³ while its mechanical strength was σ_{wall} = 471 ± 50 kPa. We recall that the subscript "wall" is used to indicate that similar in values mass density and mechanical strength are expected for the walls (the porous solid matrix) inside the porous materials produced after drying the foamed suspensions [34]. The measured values of ρ_{wall} and σ_{wall} allowed us to plot the relative mechanical strength of the porous carbonate materials, as a function of their relative mass density, and to compare the results with the data for the porous silica materials, described in Ref. [34]. As seen from Fig. 5, the dimensionless data for the two types of particles (silica and carbonate) agree very well with each other. Furthermore, for both silica and
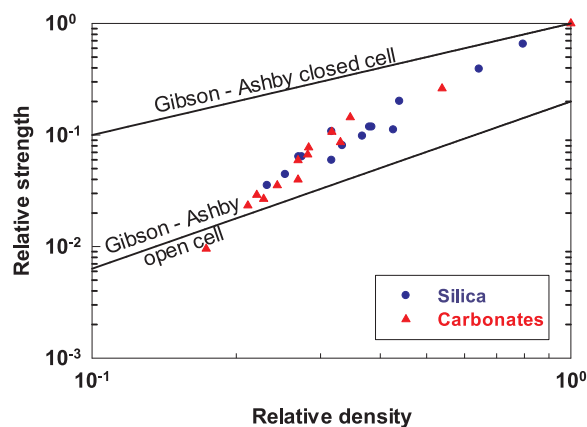

Fig. 5. Relative strength of porous silica and carbonate materials, as a function of the relative mass density of the materials. The density is scaled with the particle matrix density, and the strength is scaled with the matrix compressive strength, respectively. The solid lines are calculated using Eqs. (3) and (4).

carbonate materials we observe a smooth transition from the Gibson-Ashby theoretical predictions [40] for closed cell structure (at high mass density) towards the theoretical prediction for open cell structure (at low mass density). The Gibson-Ashby model, used to plot the solid lines in Fig. 5 implies that:

$$\frac{\sigma_{Cr}}{\sigma_{wall}} = \left(\frac{\rho}{\rho_{wall}}\right) (closed \ \ cells) \tag{3}$$

$$\frac{\sigma_{Cr}}{\sigma_{wall}} = 0.2\left(\frac{\rho}{\rho_{wall}}\right)^{1.5} (open \ \ cells) \tag{4}$$

Here, σ_{Cr} is the mechanical strength of the porous material and σ_{wall} is the respective wall (matrix) strength. The values used to plot the data in Fig. 5 for the silica dispersions are $\rho_{wall} = 474 \pm 30 \ kg/m^3$ and $\sigma_{wall} = 1463 \pm 200 \ kPa$ [34].

As seen from Fig. 4, the bubbles in some of the samples are bigger than the bubbles in others. More detailed information about the mean bubble size and bubble polydispersity is presented in the *ESI*. The comparison of the data for the bubble size with those for the mechanical strength of the respective porous materials did not reveal any correlation. For example, the bubbles in the presence of LAS are smaller than those produced in the presence of SDS but larger than those with AOT, while the mechanical strength of LAS-containing materials is higher than that for both SDS and AOT (cf. Fig. 4A). The bubbles in octanoic acid-containing foams are even bigger but the final porous materials are the strongest, due to the minimum cracks observed in this system. Also, we did not see any indications that the bubble size, the open-cell formation and/or the crack formation are directly correlated. As shown in Refs. [33–34], we can prepare materials with open cell structure without having cracks, as well as we observe cracks in materials with closed cell structures [34].

Therefore, we explained the crack formation in Ref. [34] as a manifestation of inhomogeneous local distribution of stresses (e.g. different local capillary pressures) during the drying process which could be a result of several (possibly interrelated) factors: formation of polydisperse particle aggregates, uneven propagation of the drying front, particle migration during drying, etc. The importance of these possible effects is further investigated in the following Section 3.3.

3.3. Crack formation and prevention upon drying - model experiments and discussion

To identify the mechanism of crack formation in the studied carbonate porous materials, we performed a series of model experiments, including measurements of the surface tension of the drying liquid phase, and of the zeta potential of the carbonate particles in the foamed suspensions, as well as drying of (2D) supernatant droplets and of (3D) macroscopic materials with impregnated tracer dyes.

First, we measured the surface tension of the supernatant solutions, separated from the foamed suspensions. These experiments aimed to determine the concentration of free surfactant molecules, after the introduced surfactant had been placed in contact with the carbonate particles. Therefore, the free surfactant molecules include those which have not been adsorbed on the particles surface and have not been precipitated when coming in contact with the Ca^{2+} ions, present in the carbonate suspensions.

With this aim in view, we prepared suspensions containing 30 wt% particles and 7 mM surfactant, homogenized and centrifuged them to separate a clear, equilibrated solution from the particles. We measured the equilibrium surface tension of the supernatants, obtained in this way (see Fig. 6A). The supernatant of carbonate suspension, in the absence of any surfactant added, had surface tension of $71 \pm 1 \ mN/m$ which indicated a high level of purity of the carbonate particles. C10Ac and C8Ac had relatively small effect on the surface tension: $72 \pm 1 \ mN/m$ was measured for C10Ac and $57 \pm 2 \ mN/m$ for C8Ac.

These values correspond to negligible concentration of free C10Ac left in the aqueous phase, and 3.1 mM ($\approx$ 45%) free C8Ac. These estimates from the surface tension data were confirmed by gas chromatography measurements. These concentrations of the free fatty acids in the supernatant indicate surfactant depletion, predominantly due to adsorption on the particle surface, rather than to acid precipitation as calcium soaps. Equilibrium estimates show that at least 1.1 mM of C10Ac and 8.5 mM C8Ac could be present in the supernatant, if the precipitation of calcium soaps were the only mechanism of fatty acid removal (ESI *section S3*).

In contrast, the supernatants of the other surfactants (SLES, LAS, etc.) had surface tensions in the range between 28 mN/m and 32 mN/m, corresponding to free surfactant concentrations around and above their CMC [30,31,36].

To check whether the surfactant adsorption affects the properties of the carbonate particles, we measured the particle zeta potentials, see Fig. 6B. As expected, the zeta potentials in the presence of anionic surfactants were lower, when compared to the original particle zeta potential, in the absence of surfactants. These results are in agreement with the optical observations of the foam films (Fig. 2) which revealed Pickering stabilization for all these foams.

Pourcel et al. [41] showed that formation of cracks in drying suspensions may be due to excessively high evaporation rates. Since we used different surfactants, allowing different levels of particle hydrophobization at the concentrations used (see *ESI table S3.1*) we checked whether we could detect a significant difference in the drying rates of the various foam samples. This idea originates from the observation that the hydrophobization of the particle surface could affect the rate of drying of granular materials [42]. However, our direct measurements showed that all variations of the drying rates were within the experimental error, $\approx 1.9 \pm 0.1 \ g$ of water evaporated per hour, for all samples studied (*ESI* Section 4).

We checked also whether the mechanism of drying is different for the various samples studied. Indeed, Faure and Coussot [43] showed that bentonite and kaolin clays dry in a different manner. In one case, there was a water receding front which gradually moved from the top to the bottom of the material being dried. In the other case, the air penetrated into the sample and formed air-impregnated regions around small wet clusters of particles. Because we had no access to equipment that allows us to verify these two mechanisms directly, we performed two types of model experiments to obtain indirect information about the possible differences in the drying behavior of the foams:

1. To investigate the particle interactions and motion upon drying, we observed the modes of drying of supernatant droplets, containing small carbonate particles [44,45]
2. To visualize the macroscopic flow of liquid upon drying of the porous materials, we introduced water-soluble dye in the foamed suspensions [46].

3.3.1. Drying drops

In these experiments we studied the same supernatants with redispersed carbonate particles of low concentrations, which were used for measurements of the particle zeta potentials in the presence of different surfactants. We placed 1–2 µL drops of these supernatants on glass slides and left them to evaporate under ambient conditions, while observing them with optical microscope, in transmitted light, with objectives $\times 2.5$ and $\times 50$.

Two distinct periods of drop evaporation were observed: (1) at fixed water-glass-air contact line in which the drop periphery is pinned and the drop contact angle gradually decreases with time [44,45], and (2) at constant receding contact angle in which the contact line gradually shrinks (and occasionally pins at larger particle clusters in a stick-slip jumps).

The length of the first period depended significantly on the specific surfactant. It was generally shorter for drops with lower contact angle
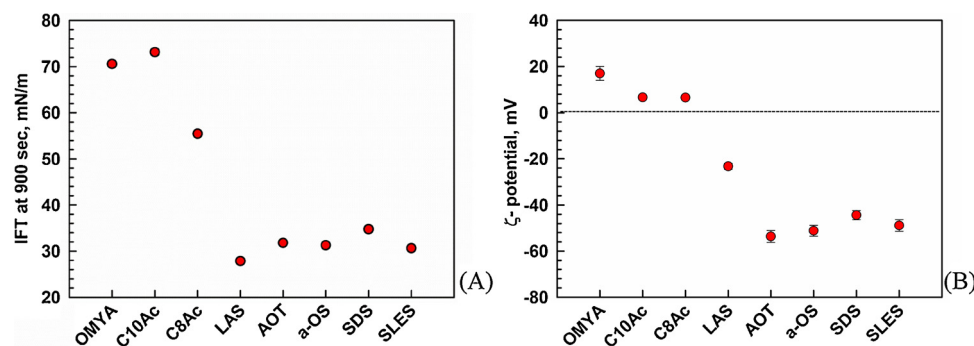
Fig. 6. Measurement of the properties of supernatant solutions, containing 30 wt% particles and 7 mM surfactant before centrifugation: **(A)** Surface tension after 900 s of measurement. **(B)** Zeta potential of 0.1 wt% particles re-dispersed from the sediment. The natural pH of the supernatant + particles is around 7.5 ± 0.5.
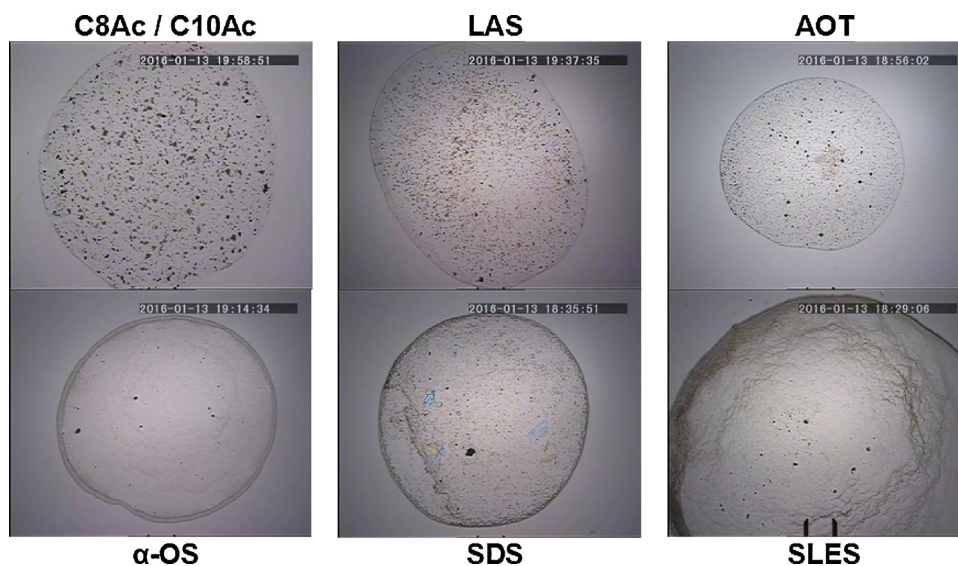

Fig. 7. Microscope images of dried supernatant droplet. The variations in the size of the dried spots are due to minor differences in the volume of the deposited drops and in the different spreading of the surfactant solutions. Scale: 400 μm.

(i.e. in the systems containing free surfactant with concentration ≥ CMC) and longer for the drops with high initial contact angle (at low concentration of the free surfactant). Along this period we observed a flux of liquid from the drop center towards its edges, causing migration of surfactant and particles, and the resulting formation of coffee rings at the drop periphery [44,45]. Illustrative movies of this process are presented in the online Supplementary videos S1-S7. The formation of "coffee" rings was more pronounced for particle aggregates with smaller size and drops with lower contact angle (lower surface tension of the solutions), viz. for SLES, SDS and α-OS surfactant solutions, see Fig. 7. The process of particle migration was somewhat slower for AOT and almost negligible for LAS and fatty acids. Small coffee rings were observed at the edge of the droplets with fatty acids, LAS and AOT, too. Notably, these rings were mostly due to local supersaturation with surfactant and formation of calcium soaps, rather than to a directed particle transport, caused by the flowing water, as it was the case for SLES, SDS and α-OS. This comparison between the systems shows that the lower in magnitude ζ-potentials, measured with C8Ac and C10Ac containing suspensions, results in more pronounced particle aggregation and sticking to the glass substrate during the drop evaporation experiment, as compared to the other surfactants (see Fig. 7).

The second period of drop evaporation led to the formation of smaller, secondary coffee rings at the temporary pinning locations of the receding contact line (see the pictures for α-OS, SDS and SLES in Fig. 7).

We observed an additional effect with the solutions containing fatty

acids. In these systems we observed the formation of a thin "skin" of calcium soap precipitates on the drop surface, along with the precipitation of small crystallites in the drop interior, as illustrated in Fig. 8. During the first period of water evaporation, small wrinkles formed at the drop periphery (*see ESI video S1*). These wrinkles were fatty acid precipitates, forming due to local supersaturation of the evaporating solutions. These wrinkles gradually grew towards the central area of the drop, forming a continuous shell on the drop surface. In the second period of the evaporation process, small rod-like crystallites of calcium precipitates with C8Ac were formed. Theoretical calculations showed that quasi-equilibrium precipitation in these drops should start after evaporating more than ca. 70% of the water in the drop (*ESI* Section 3). However, in reality, the precipitation started earlier, due to the local supersaturation at the drop periphery.

This surface precipitation could serve as an additional mechanism for crack prevention via formation of precipitation shells. The drying fronts appear first in the larger pores of the drying foams [50,51]. The increased solution flux through these pores could cause a local supersaturation of fatty acid and formation of soap shells, like those observed in the experiments with drying drops, which would "seal" the drying pores and will precipitate material in the capillary bridges, connecting the carbonate particles, thus reinforcing the contacts between these particles.

Large migrations of particles, similar to the particle transport leading to coffee ring effects, have been observed before in 3D granular media, saturated with coffee nanoparticles [47]. Such particle
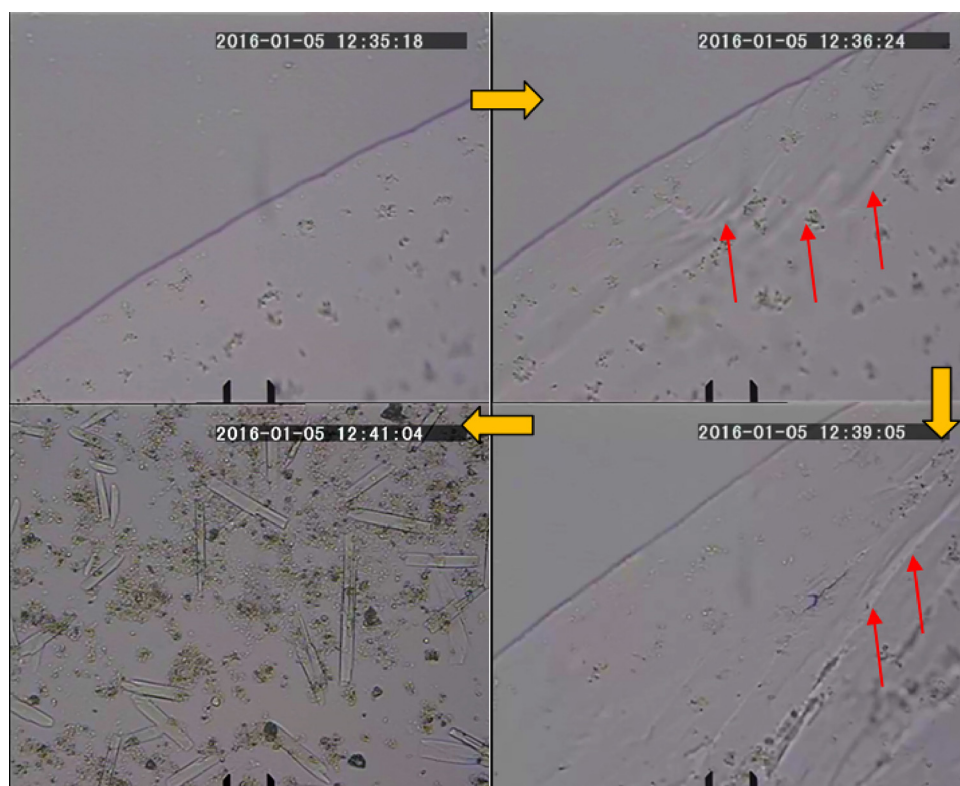
Fig. 8. Microscope images of drying supernatant droplet, containing C8Ac. After evaporating small quantity of solution, the local supersaturation of Ca(C8Ac)$_2$ causes the formation of thin precipitated shell on the drop surface, indicated by the red arrows. As the evaporation continues the shell grows from the edge towards the drop center. The rest of the surfactant precipitates in the form of small rodlike crystals in the drop center. Scale, 20 μm (For interpretation of the references to colour in this figure legend, the reader is referred to the web version of this article).

migrations could perturb significantly the homogeneous distribution of the solid material in the drying foams, thus facilitating the formation of cracks in the process of drying. Indeed, the particle accumulation in some regions, at the expense of the particle depletion in the other regions, results in non-isotropic shrinkage in the different regions of the drying foams. The capillary and mechanical stresses would be inhomogenously distributed during drying and cracks could form [48,49], like those observed in the lower part of the solidifying carbonate foams. Therefore, one could expect that the systems in which the particle migration is suppressed, should result in stronger dry materials – a hypothesis which is confirmed by our experiments, as explained below.

3.3.2. Visualization of the macroscopic liquidflow in drying porous materials

To check if the calcium soaps precipitation and the particle migration change the drying mechanism in the drying foams, we added tracer dye in the foamed suspensions [46]. We added the anionic (sulfonate) dye Eriochrome black which forms red-colored complexes in the presence of Ca^{2+} ions [52]. The solutions of Eriochrome have blue color in the absence of Ca^{2+} ions and its crystals are black.

We dissolved ≈50 μM Eriochrome in the suspensions, just before starting the foaming procedure, but after the surfactants had been added to the suspensions. Afterwards, we prepared foams with 65 vol% air and dried them at 25 ± 5 °C or at 60 ± 10 °C, in both cases at ambient humidity. The produced foams have light pinkish color immediately after their preparation (Fig. 9A), due to the formation of Eriochrome-calcium complexes with the calcium ions dissolved in the aqueous phase from the carbonate particles. After drying the foams at ambient conditions (Fig. 9B and C), we observed light homogeneous pink color on the top surface of the C8Ac material (Fig. 9B) which had the strongest mechanical properties. In contrast, the foam with SDS (Fig. 9C) had exposed inhomogeneous lighter and darker areas, which indicated inhomogeneous flow of the drying water throughout these materials.

This result was much more pronounced at the higher temperature of

drying, see Fig. 9D–E. Far more intensive coloring of the top sample surface was observed in both cases, indicating more intensive mass flux of water and dye during drying. The presence of many black spots (dry Eriochrome crystals) on the surface of the SDS materials revealed the presence of local pores in which the evaporation rate and water transport was much higher, compared to the average drying rate. In contrast, the C8Ac material was still very homogeneous and only few darker spots were seen on its surface, see Fig. 8. In addition, the materials formed with C8Ac had very similar mechanical strength after drying at different temperatures, while the materials with SDS showed worse mechanical properties when dried at higher temperature.

Thus we could link the different mechanical properties of the materials to different modes of water evaporation, depending on the surfactant studied. It is important to ensure homogeneous mode of water evaporation and to suppress the transport of particles inside the drying material via sticking to the other particles (via mild attraction) to ensure the formation of homogeneous, mechanically strong final porous material.

3.3.3. Role of suspension rheology

In our previous studies [32–34] we revealed a very important role of the suspension rheological properties (yield stress and viscosity) on the formation of stable porous materials from silica suspensions. Therefore, we checked for the possible effects of the studied surfactants on the rheological properties of the carbonate suspensions.

All suspensions, containing 30 wt % carbonate particles, with and without 7 mM surfactant, behaved as yield-stress fluids and are described well by Herschel-Bulkley model:

$$\tau = \tau_0 + K\dot{\gamma}^n \qquad (5)$$

where τ_0 is the yield stress of the suspension, K is its consistency, and n is its flow index. These characteristics of the studied suspensions are summarized in Table 2 for the different surfactants. In contrast to our previous results with silica suspensions, the studied surfactants (at 7 mM concentration) showed relatively weak effect on the rheological properties of the carbonate suspensions. The yield stress is slightly
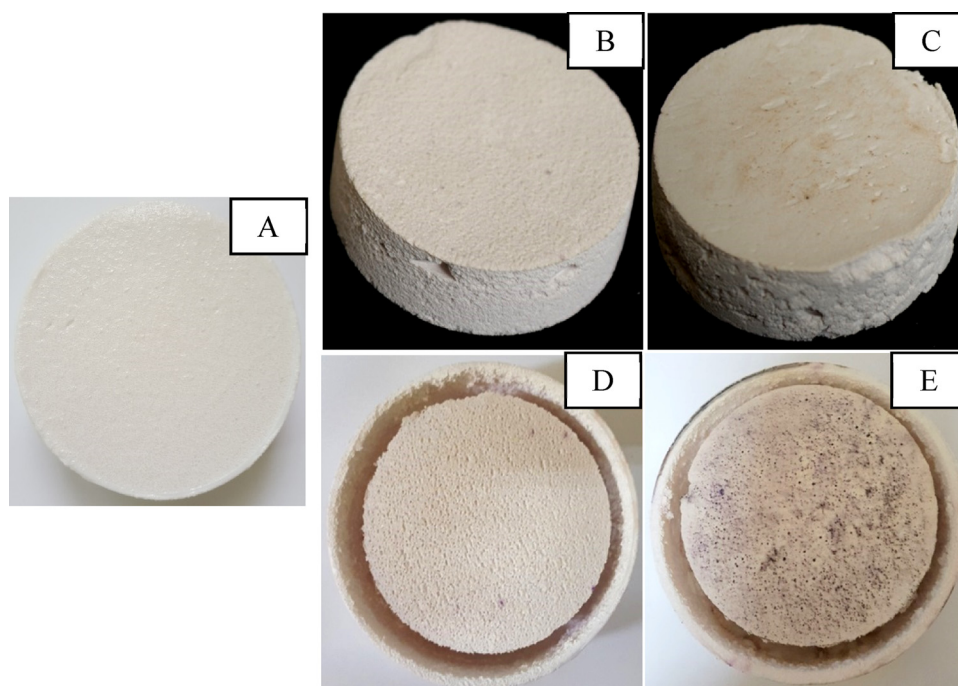
Fig. 9. Macroscopic sample of foams containing 65 vol% air and the respective dried materials: (A) Foam outlook in the presence of ≈ 50 µM Eriochrom black T, just before drying. The respective materials obtained in the presence of 7 mM C8Ac (B and D) or SDS (C and E). The materials shown in (B) and (C) are dried at 25 ± 5 °C, while those shown in (D) and (E) are dried at 60 ± 10 °C.

Table 2

Rheological properties of the carbonate suspensions (± surfactant), and their viscosity at the shear rate of foaming. The parameters are extracted using Herschel-Bulkley model for suspensions sheared between 100 and 2000 s^{-1}.

System	τ_0, Pa	K	n	Viscosity at 100s^{-1}, mPa.s
30 wt.% particles	7.4	0.62	0.52	112.0
+ C8Ac	8.5	0.14	0.65	92.0
+ C10Ac	10.6	0.71	0.47	135.6
+ SLES-3EO	8.5	0.31	0.55	136.5
+ LAS	11.3	1.23	0.40	178.5

increased for LAS and decanoic acid only, and the apparent viscosity at the shear rate of foaming is significantly increased for LAS only.

This difference in the surfactant effect on the rheological behavior of the silica and carbonate suspensions is due to the much lower surface area and the lower surface charge of the carbonate particles, as compared to silica particles. Indeed, we used nearly 90 times less surfactant, defined as the surface coverage of the particles (0.38 µg/m^2 for carbonates vs. 33 µg/m^2 for silica) to ensure most appropriate conditions for foaming and for production of stable dry carbonate porous materials. This very low particle surface coverage leads to low particle hydrophobization and, hence, to weak effect on the suspension rheology. Therefore, we conclude from these results that the main role of the surfactants in the carbonate suspensions is to ensure Pickering stabilization of the foams, while their effect on the suspension rheological properties is secondary.

In comparison, for silica suspensions, the role of the cationic surfactant TTAB was to simultaneously ensure Pickering stabilization of the foams and sufficiently high yield stress of the suspensions, whereas the role of the zwitterionic surfactant CAPB was to modify the suspension rheological properties and, simultaneously, to stabilize the foam films between the neighboring bubbles [34].

Thus we see some subtle differences between the suspensions of the various types of particles, while the main principles of stabilization remain similar. Based on all our experiments with silica and carbonate suspensions we reinforce our conclusions [34] that the general requirements for preparation of crack-free porous materials from foam precursors are: (1) to have a "mild" attraction between the neighboring particles which is detected as a moderate yield stress of the

suspension, (2) lack of strong particle aggregation, and (3) propagation of homogeneous water front during foam drying. In the current study, these requirements are met by the carbonate suspensions containing fatty acids. We observe an appropriate yield stress for all carbonate suspensions, but it is not affected significantly by the various surfactants. Therefore, the suspensions containing fatty acids differ mostly in the local precipitation of calcium soaps during drying which ensures more homogeneous drying front and, as explained above, thus facilitates the formation of crack-free materials.

4. Conclusions

Eight surfactants, reported in the literature to modify CaCO$_3$ surface, are compared in their ability to assist the formation of crack-free, solid carbonate porous materials with tunable mass density and mechanical properties. The most important results could be summarized as follows:

In situ surface modification of the positively charged CaCO$_3$ particles is achieved by a variety of anionic surfactants, as long as they have a solubility product with the Ca^{2+} ions $pK_{SP} \leq 9.5$ (the Ca^{2+} ions are dissolved from the surface of the carbonate particles).

The wet foams, obtained in the presence of anionic surfactants or fatty acids, are stable to water drainage and Ostwald ripening, but most of them crack upon drying. Detailed analysis showed that, despite the lack of severe aggregation and the lower capillary pressures in the drying foams containing SDS, SLES, LAS and a-OS as surfactants, these foams have lower mechanical strength and crack severely upon drying. In contrast, the fatty acids with C8 and C10 chains are very efficient for preparing crack-free and mechanically strong porous carbonate materials.

The ability of the fatty acids to reduce cracks formation is explained mechanistically with their specific effects on the drying process. The fatty acids suppress the particle migration along the pores of the drying material. In addition, the supersaturation of the drying aqueous phase with calcium soaps leads to local precipitation of these soaps in the larger pores, which results in a partial pore sealing with precipitated material and in the development of more homogeneous drying front. As a result, the particle distribution and the shrinkage of the drying material are more homogeneous in these samples. The precipitation of

calcium soaps in the drying contact zones between the neighboring carbonate particles (viz. in the liquid capillary bridges formed between the carbonate particles in the final stage of material drying) may further reinforce the dry porous materials.

Appendix A. Supplementary data

Supplementary material related to this article can be found, in the online version, at doi:https://doi.org/10.1016/j.colsurfa.2018.05.025.

References

[1] P. Colombo, Conventional and novel processing methods for cellular ceramics, Philos. Trans. R. Soc. A 364 (2006) 109–124.

[2] S. Dhara, P. Bhargava, Influence of slurry characteristics on porosity and mechanical properties of alumina foams, Int. J. Appl. Cer. Technol. 3 (2006) 382–392.

[3] U. Gonzenbach, A. Studart, E. Tervoort, L. Gauckler, Tailoring the microstructure of particle-stabilized wet foams, Langmuir 23 (2007) 1025–1032.

[4] U. Gonzenbach, A. Studart, E. Tervoort, L. Gauckler, Ultrastable particle-stabilized foams, Angew. Chem. Int. Ed. 45 (2006) 3526–3530.

[5] K. Velikov, F. Durst, O. Velev, Direct observation of the dynamics of latex particles confined inside thinning water-air films, Langmuir 14 (1998) 1148–1155.

[6] N. Denkov, I. Ivanov, P. Kralchevsky, D. Wasan, A possible mechanism of stabilization of emulsions with solid particles, J. Colloid Interface Sci. 150 (1992) 589–593.

[7] G. Kaptay, Interfacial criteria for stabilization of liquid foams by solid particles, Colloids Surf. A 230 (2003) 67–80.

[8] Z. Du, M. Bilbao-Montoya, B. Binks, E. Dickenson, R. Ettelaie, B. Murray, Outstanding stability of particle-stabilized bubbles, Langmuir 19 (2003) 3106–3108.

[9] E. Dickinson, R. Ettelaie, T. Kostakis, B. Murray, Factors controlling the formation and stability of air bubbles stabilized by partially hydrophobic silica nanoparticles, Langmuir 20 (2004) 8517–8525.

[10] B. Binks, T. Horozov, Aqueous foams stabilized solely by silica nanoparticles, Angew. Chem. Int. Ed. 44 (2005) 3722–3725.

[11] B. Binks, R. Murakami, Phase inversion of particle-stabilized materials from foams to dry Water, Nat. Mater. 5 (2006) 865–869.

[12] G. Kaptay, On the equation of the maximum capillary pressure induced by solid particles to stabilize emulsions and foams and on the emulsion stability diagrams, Colloids Surf. A 282 (2006) 387–401.

[13] U. Gonzenbach, A. Studart, E. Tervoort, L. Gauckler, Stabilization of foams with inorganic colloidal particles, Langmuir 22 (2006) 10983–10988.

[14] B. Binks, M. Kirkland, J. Rodrigues, Origin of stabilisation of aqueous foams in nanoparticle–surfactant mixtures, Soft Matter 4 (2008) 2373–2382.

[15] S. Zhang, Q. Lan, Q. Liu, J. Xu, D. Sun, Aqueous foams stabilized by laponite and CTAB, Colloids Surf. A 317 (2008) 406–413.

[16] S. Zhang, D. Sun, X. Dong, C. Li, J. Xu, Aqueous foams stabilized with particles and nonionic surfactants, Colloids Surf. A 324 (2008) 1–8.

[17] Q. Liu, S. Zhang, D. Sun, J. Xu, Aqueous foams stabilized by hexylamine-modified laponite particles, Colloids Surf. A 338 (2009) 40–46.

[18] X. Dong, J. Xu, C. Cao, D. Sun, X. Jiang, Aqueous foam stabilized by hydrophobically modified silica particles and liquid paraffin droplets, Colloids Surf. A 353 (2010) 181–188.

[19] Q. Liu, S. Zhang, D. Sun, J. Xu, Foams stabilized by laponite nanoparticles and alkylammonium bromides with different alkyl chain lengths, Colloids Surf. A 355 (2010) 151–157.

[20] N. Vilkova, S. Elaneva, P. Kruglyakov, O. Dorchina, Influence of the structure-net in the continuous phase of the foam stabilized by solid particles on the foam properties, Reg. Archit. Eng. (in Russian) 2 (9) (2010) 20–30.

[21] L. Arriaga, W. Drenckhan, A. Salonen, J. Rodrigues, R. Íñiguez-Palomares, E. Rio, D. Langevin, On the long-term stability of foams stabilised by mixtures of nanoparticles and oppositely charged short Chain surfactants, Soft Matter 8 (2012) 11085–11097.

[22] A. Maestro, E. Rio, W. Drenckhan, D. Langevin, A. Salonen, Foams stabilised by mixtures of nanoparticles and oppositely charged surfactants: relationship between

[23] E. Rio, W. Drenckhan, A. Salonen, D. Langevin, Unusually stable liquid foams, Adv. Colloid Interface Sci. 205 (2014) 74–86.

[24] P. Somasundaran, G. Agar, The zero Point of charge of calcite, J. Colloid Interface Sci. 24 (4) (1967) 433–440.

[25] J. Hanna, I. Anazia, Fatty acid separation of siliceous carbonate phosphates, Mine. Metall. Proc. 7 (2) (1990) 84–89.

[26] J. Hanna, I. Anazia, Innovative process for beneficiation of dolomitic phosphate ores int, J. Miner. Process. 23 (3–4) (1988) 311–314.

[27] J. Hanna, I. Anazia, New flotation approach for carbonate phosphate separation, Min.. Metall. Proc. 4 (4) (1987) 196–202.

[28] M.A. Osman, U.W. Suter, Surface treatment of calcite with fatty acids: structure and properties of the organic monolayer, Chem. Mater. 14 (2002) 4408–4415, http://dx.doi.org/10.1021/cm021222u.

[29] W. Zhou, J. Cao, W. Liu, S. Stoyanov, How rigid rods self-assemble at curved surfaces, Angew. Chem. Int. Ed. 48 (2009) 378–381, http://dx.doi.org/10.1002/anie.200804194.

[30] Z.-G. Cui, Y.-Z. Cui, C.-F. Cui, Z. Chen, B.P. Binks, Aqueous foams stabilized by in situ surface activation of CaCO3 nanoparticles via adsorption of anionic surfactant, Langmuir. 26 (2010) 12567–12574, http://dx.doi.org/10.1021/la1016559.

[31] E. Song, D. Kim, B.J. Kim, J. Lim, Surface modification of CaCO3 nanoparticles by alkylbenzene sulfonic acid surfactant, colloids surfaces a physicochem, Eng. Asp. 461 (2014) 1–10, http://dx.doi.org/10.1016/j.colsurfa.2014.07.020.

[32] I. Lesov, S. Tcholakova, N. Denkov, Drying of particle-loaded foams for production of porous materials: mechanism and theoretical modeling, RSC Adv. 4 (2014) 811–823.

[33] I. Lesov, S. Tcholakova, N. Denkov, Factors controlling the formation and stability of foams used as precursors of porous materials, J. Colloid Interface Sci. 426 (2014) 9–21.

[34] I. Lesov, S. Tcholakova, M. Kovadjieva, T. Saison, M. Lamblet, N. Denkov, roles of role of Pickering stabilization and bulk gelation for the preparation and properties of solid silica foams, J. Colloid Interface Sci. 504 (2017) 48–57, http://dx.doi.org/10.1016/j.jcis.2017.05.036.

[35] C. Chuanuwatanakul, C. Tallon, D. Dunstan, G. Franks, Controlling the microstructure of ceramic particle stabilized foams: influence of contact angle and particle aggregation, Soft Matter 7 (2011) 11464–11474.

[36] Z.-G. Cui, C.-F. Cui, Y. Zhu, B.P. Binks, Multiple phase inversion of emulsions stabilized by in situ surface activation of CaCO3 nanoparticles via adsorption of fatty acids, Langmuir 28 (2012) 314–320, http://dx.doi.org/10.1021/la204021v.

[37] R.R. Irani, C.F. Callis, Metal complexing by phosphorous compounds. II. solubilities of calcium soaps of linear carboxylic acids, J. Phys. Chem. 64 (11) (1960) 1741–1743, http://dx.doi.org/10.1021/j100840a034.

[38] H. Zhang, C.A. Miller, P.R. Garrett, K.H. Raney, Defoaming effect of calcium soap, J. Colloid Interface Sci. (2004) 539–547, http://dx.doi.org/10.1016/j.jcis.2004.06.103.

[39] Q. Jin, P. Tan, A.B. Schofield, Lei Xu, Eliminating cracking during drying, Eur. Phys. J. E 36 (28) (2013), http://dx.doi.org/10.1140/epje/i2013-13028-9.

[40] L. Gibson, M. Ashby, The mechanics of foams: basic results, Cellular Solids: Structure and Properties, Cambridge University Press, Cambridge, 1997, pp. 175–234, http://dx.doi.org/10.1017/CBO9781139878326.007 Cambridge Solid State Science Series.

[41] F. Pourcel, W. Jomaa, J.-R. Puiggali, L. Rouleau, Criterion for crack initiation during drying: alumina porous ceramic strength improvement, Powder Technol. 172 (2007) 120–127, http://dx.doi.org/10.1016/j.powtec.2006.10.041.

[42] N. Shahidzadeh-Bonn, A. Azouni, P. Coussot, Effect of wetting properties on the kinetics of drying of porous media, J. Phys. Condens. Matter 19 (2007) 112101, http://dx.doi.org/10.1088/0953-8984/19/11/112101.

[43] P. Faure, P. Coussot, Drying of a model soil, Phys. Rev. E. 82 (2010) 036303, , http://dx.doi.org/10.1103/PhysRevE.82.036303.

[44] U.U. Ghosh, M. Chakraborty, A.B. Bhandari, S. Chakraborty, S. DasGupta, Effect of surface wettability on crack dynamics and morphology of colloidal films, Langmuir 31 (2015) 6001–6010, http://dx.doi.org/10.1021/acs.langmuir.5b00690.

[45] J.Y. Kim, K. Cho, S. Ryu, S.Y. Kim, B.M. Weon, Crack formation and prevention in colloidal drops, Sci. Rep. 5 (2015) 13166, http://dx.doi.org/10.1038/srep13166.

[46] N. Shokri, D. Or, Drying patterns of porous media containing wettability contrasts, J. Colloid Interface Sci. 391 (2013) 135–141, http://dx.doi.org/10.1016/j.jcis.2012.08.074.

[47] E. Keita, P. Faure, S. Rodts, P. Coussot, MRI evidence for a receding-front effect in drying porous media, Phys. Rev. E 87 (2013) 062303, , http://dx.doi.org/10.1103/PhysRevE.87.062303.

[48] E. Keita, S.A. Koehler, P. Faure, D.A. Weitz, P. Coussot, Drying kinetics driven by the shape of the air/water interface in a capillary channel, Eur. Phys. J. E 39 (2016) 23, http://dx.doi.org/10.1140/epje/i2016-16023-8.

[49] Y. Xu, G.K. German, A.F. Mertz, E.R. Dufresne, Imaging stress and strain in the fracture of drying colloidal films, Soft Matter 9 (2013) 3735, http://dx.doi.org/10.1039/c3sm27912j.

[50] P. Coussot, Scaling approach of the convective drying of a porous medium, Eur. Phys. J. B 15 (2000) 557–566, http://dx.doi.org/10.1007/s100510051160.

[51] J. Thiery, S. Rodts, E. Keita, X. Chateau, P. Faure, D. Courtier-Murias, et al., Water transfer and crack regimes in nanocolloidal gels, Phys. Rev. E - Stat. Nonlinear, Soft Matter Phys. 91 (2015) 042407, , http://dx.doi.org/10.1103/PhysRevE.91.042407.

[52] A. Young, T.R. Sweet, Complexes of eriochrome Black T with calcium and magnesium, Anal. Chem. 27 (1955) 418–420, http://dx.doi.org/10.1021/ac60099a026.